

## Detector Challenges of the strong-field QED experiment LUXE at the European XFEL

---

**Arka Santra<sup>a,\*</sup> on behalf of the LUXE Collaboration**

<sup>a</sup>*Weizmann Institute of Science,,  
234 Herzl Street, Rehovot, Israel*

*E-mail: [arka.santra@weizmann.ac.il](mailto:arka.santra@weizmann.ac.il)*

The LUXE experiment aims at studying high-field QED in electron-laser and photon-laser interactions, with the 16.5 GeV electron beam of the European XFEL and a laser beam with power of up to 350 TW. This experiment will use one electron bunch out of 2700 bunches per train from XFEL. The experiment will measure the multiplicity spectra of electrons, positrons and photons in expected ranges of  $10^{-3}$  to  $10^9$  particles per 1 Hz bunch crossing, depending on the laser power and focus. These measurements have to be performed in the presence of low-energy high radiation-background. To meet these challenges, for high-rate electron and photon fluxes, the experiment will use Cherenkov radiation detectors, scintillator screens, sapphire sensors as well as lead-glass monitors for backscattering off the beam-dump. A four layer silicon-pixel tracker and a compact electromagnetic tungsten calorimeter with GaAs sensors will be used to measure the positron spectra. The layout of the experiment and the expected performance under the harsh radiation conditions will be presented. Beam tests for the Cherenkov detector and the electromagnetic calorimeter were performed at DESY recently and results will be presented. The experiment received a stage 1 critical approval (CD1) from the DESY management and is in the process of preparing its technical design report (TDR). It is expected to start running in 2025/6.

*10th International Workshop on Semiconductor Pixel Detectors for Particles and Imaging (Pixel2022),  
12-16 December 2022  
Santa Fe, New Mexico, USA*

---

\*Speaker

## 1. Introduction

Quantum Electrodynamics (QED) is the theory of relativistic quantum field theory of electrodynamics. Although QED is well-understood in the perturbative regime, it is not well understood in the strong field regime. The Schwinger critical field, denoted by  $\mathcal{E}_{\text{cr}} \equiv m_e^2 c^3 / e \hbar = 1.32 \times 10^{18}$  V/m, where  $m_e$  and  $e$  are electron mass and charge, respectively, characterizes the strong field regime of QED (SFQED in short). This strong electric field is capable of producing electron and positron pairs from the vacuum. This strong field is not achievable statically in terrestrial laboratories, however the collision of modern day ultra-intense laser beam and highly energetic electron or photon beam helps to probe this regime. Two of the strong field phenomena, non-linear Compton scattering and laser assisted  $e^+e^-$  pair production, have been studied extensively theoretically [1, 2]. These processes are represented by the following equations, respectively:

$$e^- + n\gamma_L \rightarrow e^- + \gamma \quad (1a)$$

$$\gamma + n\gamma_L \rightarrow e^+ + e^-, \quad (1b)$$

where  $n$  represents the number of laser photons ( $\gamma_L$ ) participating in the process.

The dimensionless parameter like laser intensity parameter ( $\xi$ ), defined by

$$\xi = \frac{e\mathcal{E}_L}{m_e c \omega_L} = \frac{m_e c^2 \mathcal{E}_L}{\hbar \omega_L \mathcal{E}_{\text{cr}}}, \quad (2)$$

where  $\mathcal{E}_L$  is the rms value of the laser electric field and  $\omega_L$  is the frequency of the laser, characterizes the interaction of the photon or the electron with the laser electric field. Another dimensionless parameter,  $\chi$ , describes the interaction or the electron recoil. This is defined by

$$\chi = \frac{e\hbar}{m_e^3 c^5} \sqrt{(F_{\mu\nu} p^\nu)^2}, \quad (3)$$

with  $F_{\mu\nu}$  the field tensor, and  $p^\nu$  the four momentum of the high energetic particle. Considering the electric field in the particle's rest frame ( $\mathcal{E}^*$ ), this equation can be rewritten as

$$\chi = \frac{\mathcal{E}^*}{\mathcal{E}_{\text{cr}}}. \quad (4)$$

The theoretical studies in SFQED started since 1930s, but the first experimental approach to study this regime was done by E144 [3, 4] in the late 90s. This experiment, based at SLAC, Stanford, studied the non-linear Compton scattering and laser assisted  $e^+e^-$  production. This experiment reached values up to  $\xi = 0.34$ .

Some other experiments, like Astra-Gemini laser facility [5, 6] also studied this region. There are few more experiments, European Extreme Light Infrastructure (ELI) [7] and LUXE [8–10] that are planned to study SFQED. The parameter space where these experiments reached or are expected to reach is summarized in fig. 1. Modern day ultra-intense laser technologies is hugely helpful in investigating uncharted territories in  $\xi$  and  $\chi$  experimentally.

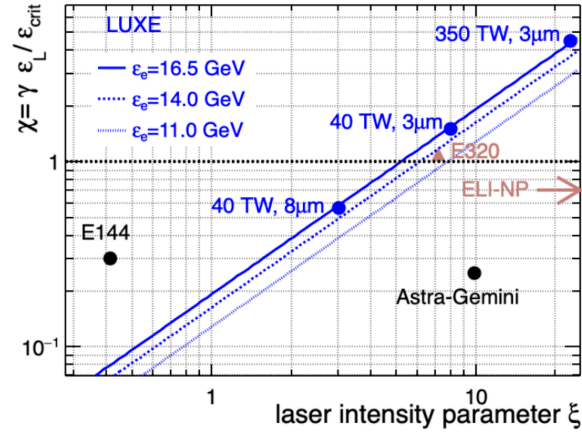


**Figure 1:** The parameter space defined by  $\chi$  vs  $\xi$  parameters as probed by various experiments. Three blue lines corresponding to different electron beam energies show the LUXE reach in this space. The phase-0 running of LUXE will use 40 TW laser, and later it will be upgraded to 350 TW laser (phase-1).

## 2. The LUXE experiment

Looking at Eq. 1, one can understand that the outgoing particles coming out of the strong field interaction between electron or photon beam with strong laser photons are electron, positron and photon. The LUXE experiment needs to detect and measure their kinematic properties in order to properly reconstruct one event. This goal drives the plan behind the LUXE detector setup. The different subdetectors of LUXE can be divided into three broad categories:

1. Positron detection system,
2. Electron detection system,
3. Photon detection system.

Initial particles in Eq. 1 are photon and electron, hence LUXE will run in both  $e$ -laser and  $\gamma$ -laser mode. In this proceeding, the  $e$ -laser setup will be described; details about  $\gamma$ -laser setup can be found in Ref. [9].

LUXE  $e$ -laser setup is outlined in fig. 2. As can be inferred from the name of the setup, the high energetic electron beam coming from XFEL [11] linear accelerator will collide with the intense laser pulse at the interaction point (IP). The interaction will happen in a vacuum chamber called interaction chamber.

## 3. The LUXE detector systems

### 3.1 Positron detection system

The laser intensity in the LUXE experiment can be easily changed by changing the laser beam waist (defined by the full-width at half maximum, FWHM, of the laser beam). This parameter dictates the rate of the outgoing particles. Depending on this parameter, the expected number of

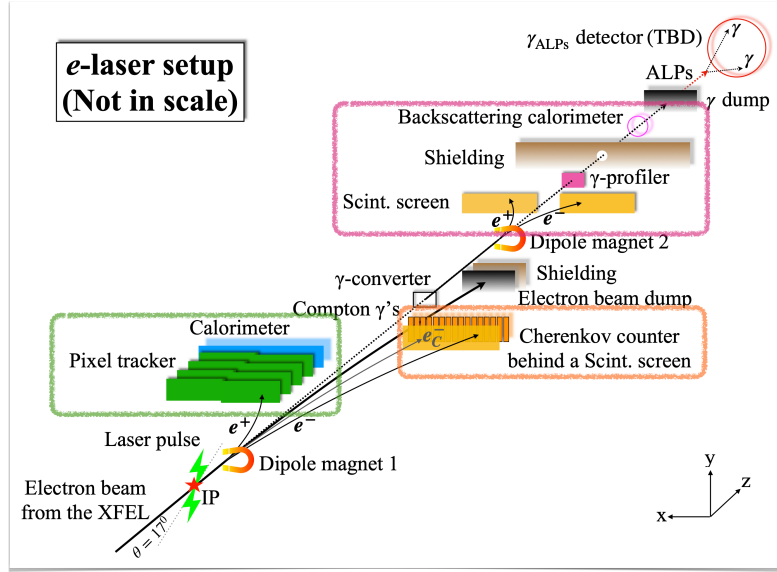


**Figure 2:** Schematic diagram of LUXE Detector Layout ( $e$ -laser mode). The different subdetector systems are marked in different colors: the positron detection system in green, the electron detection system in orange and the photon detection system in pink. The Axion-like particles (ALP), one of the postulated beyond Standard Model particles, detection system is shown at the very end, - however detector technology for this part is not yet finalized.

positrons per bunch crossing (BX) can vary from  $10^{-2}$  to  $10^5$ . The challenge for the positron detection system is then to have an excellent positron detection efficiency in a wide range of signal multiplicity, despite the presence of high background. In the LUXE experiment, most of the background comes from the original electron beam (with  $1.5 \times 10^9$  electrons per BX) getting dumped in the experimental area. The positron detection efficiency contains a silicon pixel tracker and an electromagnetic calorimeter, both systems perform well in rejecting background particles in the low signal rate regions.

The tracker detector will consist of ALPIDE pixel sensors. These sensors are jointly developed by the ALICE Collaboration [12] along with Tower Semiconductor [13]. The tracker detector will have four layers, each layer made of two staves. Each staff will have 9 pixel chips, where each chip has  $512 \times 1024$  pixels. The dimension of each pixel is  $27 \times 29 \mu\text{m}^2$ . The spatial resolution of this detector system is  $5 \mu\text{m}$ . The tracking efficiency is more than 95% for particle energy  $> 2.5 \text{ GeV}$  with an energy resolution better than  $\sim 1\%$ . The tracking efficiency and energy resolution for one signal sample ( $\xi = 3$ ) is shown in fig. 3.

Beyond the tracker subdetector system, there will be an electromagnetic calorimeter which will be a sampling calorimeter. This sampling calorimeter consists of 20 layers of tungsten plate of thickness  $3.5 \text{ mm}$  ( $1 X_0$ ). The sensor planes will be kept in between the absorber plates within  $1 \text{ mm}$  gap. The structure will have support from aluminum frame having slots on top. These slots will accommodate the front-end boards.

Silicon sensors with  $320 \mu\text{m}$  thickness with pad dimension  $5.5 \times 5.5 \text{ cm}^2$  will be used in the calorimeter. Each pad has 256 sensors. The surface area will be  $9 \times 9 \text{ cm}^2$  and length in  $x$  will be  $54 \text{ cm}$ . In the high signal rate region, where single positron showers overlap, high granularity in

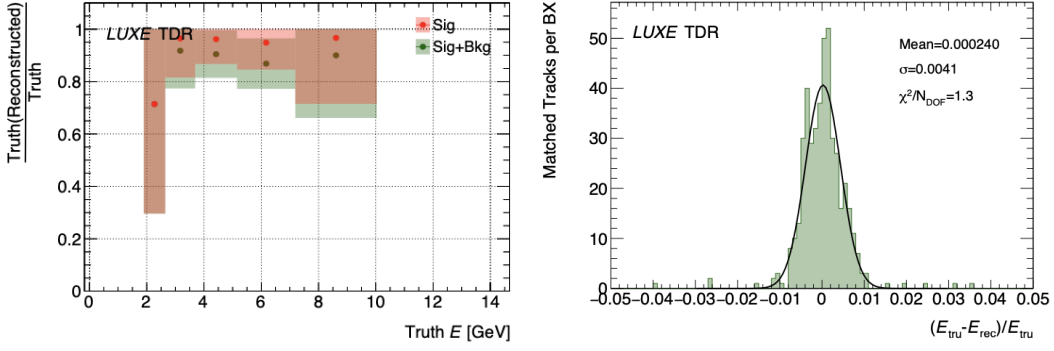


**Figure 3:** The positron reconstruction efficiency as a function of true energy is shown for signal sample with  $\xi = 3$  (left). The energy resolution of this signal in presence of background is shown on the right. This is fit with a Gaussian. The fit parameters are also shown.

the electromagnetic calorimeter proves very useful in providing the energy spectrum.

In fig. 4, the relative energy resolution as well as the position resolution of the calorimeter is shown.

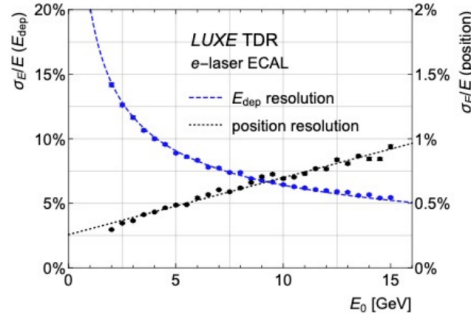


**Figure 4:** The relative energy resolution as well as the position resolution of the electromagnetic calorimeter as a function of the positron energy.

A schematic diagram of the pixel tracker and electromagnetic calorimeter is given in fig. 5.

### 3.2 Electron detection system

For the LUXE experiment, the electrons need not be reconstructed at a single particle level; here only the particle flux is important. The distribution of the electron energy is reconstructed from the electron flux. This drives the technology in the electron detection system.

The electron particle flux in the  $e$ -laser mode of LUXE is very high, of the order of  $10^9$  per BX. The electron detection system of LUXE consists of a Cherenkov detector and a scintillator screen, which are able to handle very high particle flux.

The scintillator screen is made of a Lanex (Tb-doped Gadolinium Oxysulfide) screen which is very radiation hard (up to 10 MGy). It will be mainly used to measure the low particle flux and low energetic spectrum of the electrons. This screen is capable of a high position resolution, as this will be coupled with CMOS camera which will take pictures of the light emitted from the scintillator screen. The position resolution of this system is  $O(100\mu\text{m})$  at  $\sim 50$  MeV.

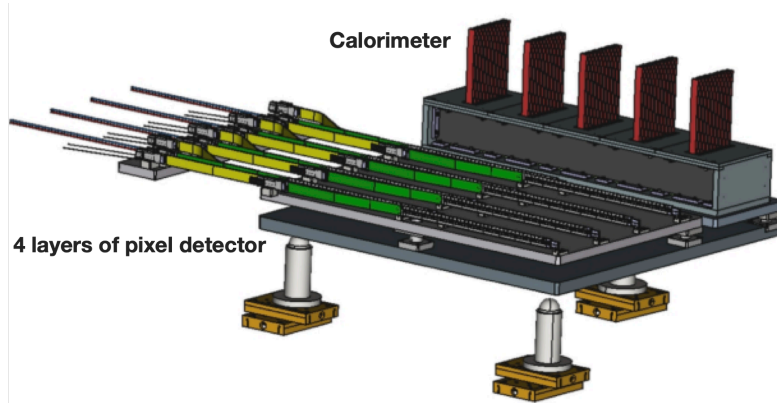


**Figure 5:** A schematic layout of the positron detection system of LUXE experiment. Here four layers of tracker made of ALPIDE chips are followed by a sampling electromagnetic calorimeter. The front end electronics will be positioned on the slots kept at the top of the electromagnetic calorimeter.

The Cherenkov detectors placed behind the screen are capable of detecting electrons with a high particle flux. Hence it complements the Lanex screen. These detectors offer a greater resistance to background particles, having low energy. Thus they are useful for the challenges of a high particle flux if a refractive medium is selected carefully. The refractive medium will be air which will be kept inside the straw tube channels. In fig. 6, the number of electrons reconstructed and the number of true electrons are shown. The reconstructed number nicely follows the true number.

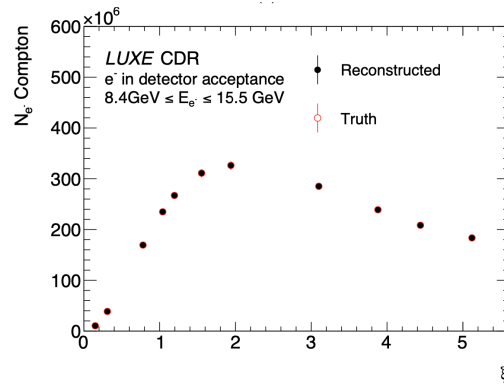


**Figure 6:** Number of Compton electrons shown as a function of  $\xi$ . The uncertainty includes the statistical uncertainty corresponding to 1 h of data taking and a systematic uncertainty on the response calibration of 2.5%. Only the electrons within a fiducial volume of 8.4 GeV to 15.5 GeV is shown as the detector has finite acceptance.

The electron detection system is shown in fig. 7.

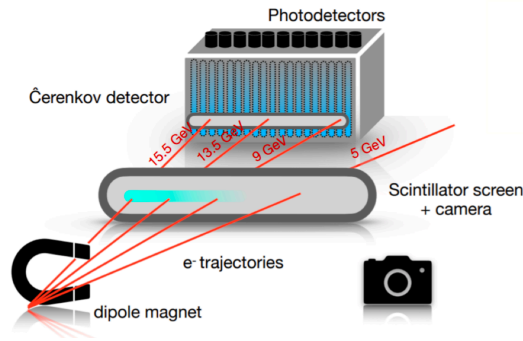


**Figure 7:** The electron detection system of LUXE. It consists of a scintillator screen and Cherenkov detector. The light profile from the scintillator screen is imaged with an optical camera. The Cherenkov light will be reflected to an array of photodetectors.

### 3.3 Photon detection system

The photon detection system is kept downstream from the interaction point. This is because the photons produced at the IP will not be deflected by the magnetic field. The photon detection system comprises of a Gamma Spectrometer, Gamma Profiler and Gamma Flux Monitor. The Gamma Spectrometer will measure the photon energy spectrum, the Gamma Profiler will measure the angular distribution. The Gamma Flux Monitor will measure the photon flux.

The Gamma Spectrometer of the photon detection system of the LUXE experiment needs to measure the energy of the high flux gamma ray beams. At the same time, it should not block the photon beams significantly so that other parts of the photon detection system can work properly. These requirements drive the technology behind the Gamma Spectrometer. It has a small tungsten target which converts photons in  $e^+e^-$ . A dipole magnet will separate the  $e^+$  and  $e^-$ . The energy of them is measured by Lanex screen coupled with CCD camera, from the position of the  $e^+$  and  $e^-$  on the screen.

In addition to the photon beam energy, LUXE needs to measure the photon beam profile as well. The beam profile will provide a straightforward and effective way to monitor the shot-by-shot stability of the laser light in its interaction with the electron or gamma beams. This online information will be important for the LUXE running and commissioning. The Gamma Profiler needs to be very radiation hard, as all of the photon beam will fall on to it. Keeping this in mind, the beam profiler will be made of sapphire which are expected to withstand up to 100 MGy. Two sapphire strip detectors placed perpendicularly will measure the size of the photon beam in horizontal and transverse plane. They have the dimension of  $2 \times 2 \text{ cm}^2$ . The thickness of them is  $100 \mu\text{m}$  and the strip pitch is  $100 \mu\text{m}$ . The beam profile distribution in  $x$  direction is shown in fig. 8. The beam profile is fit with a Cauchy-Lorentz distribution and also a simple Gaussian distribution. The fits are overlaid on the distribution.

The energy spectra normalization needs to know the particle fluxes on an event-by-event basis.

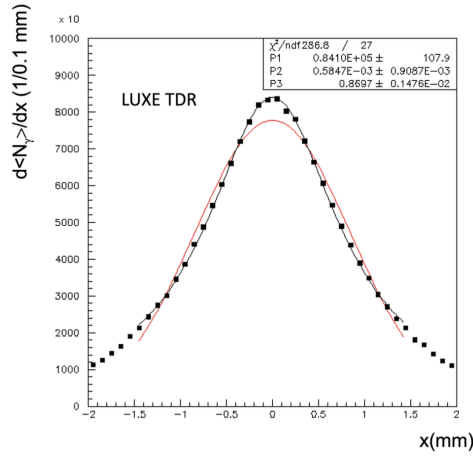


**Figure 8:** Beam profile of photons impinging the first station of sapphire detector for  $\xi = 5$ , showing the profile in  $x$  direction. The black line shows the profile fit with a Cauchy-Lorentz distribution whereas the red line shows a fit with a Gaussian distribution.

This, along with the angular distributions of photons, will be provided by the Gamma Flux Monitor. This flux monitor cannot be kept near the interaction point as there will be positrons and electrons along with the photons. The flux monitor needs to be kept further downstream so that the electrons and positrons cannot reach there. The technology here measures the energy flow of back-scattered photons from the beam dump kept at the end of the beam line. This system, basically a backscattering calorimeter, consists of 8 lead glass blocks around the beam axis having a radius of  $\sim 17$  cm. There is a linear dependence between the energy deposited in the calorimeter and the number of incident photons on the calorimeter. This is shown in fig. 9.

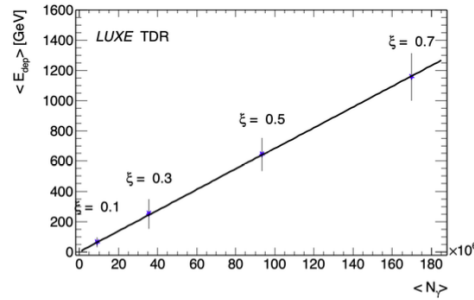


**Figure 9:** Average energy deposition as a function of the mean number of photons measured at the backscattering calorimeter. The different laser intensity parameter ( $\xi$ ) used for the plot is mentioned.

Fig. 10 shows the schematic diagrams of the Gamma Spectrometer and the backscattering calorimeter of the photon detection system.

#### 4. Conclusion

The LUXE experiment will explore the uncharted region of SFQED. This will be done with the help of multi-terawatt high intensity laser and a high energetic electron beam from the European

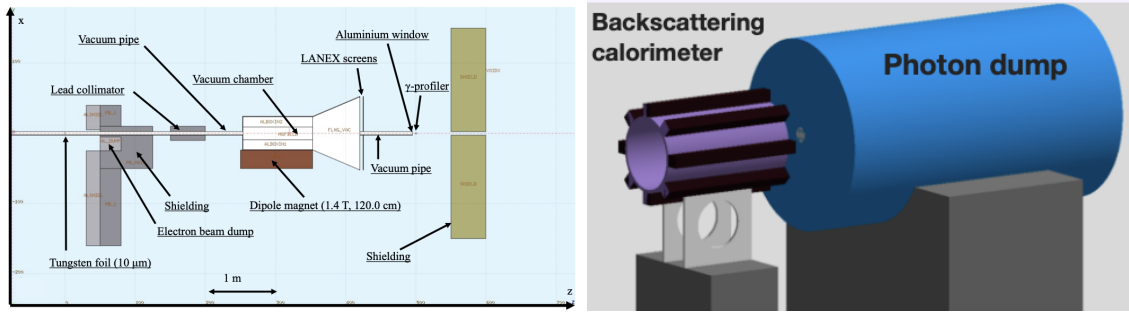


**Figure 10:** Different components of the Gamma Spectrometer (left) and the backscattering calorimeter with the photon dump (right).

XFEL. This regime is relevant for a variety of atomic physics, high energy accelerators and astrophysical phenomena. The LUXE subdetectors are designed to achieve a high signal efficiency and a good background rejection, where the signal rate varies from  $10^{-2}$  to  $10^9$  per BX. This experiment will use dipole magnets, tracker detectors made of ALPIDE chips, calorimeters made of silicon sensors, Cherenkov counters, Lanex screens, Sapphire strip detectors and a backscattering calorimeter made of lead glass blocks. They will provide the required signal efficiency as well as very good background rejection. This experiment received a stage 1 critical improvement (CD1) from the DESY management. At present, it is in the process of preparing a technical design report (TDR). The installation of these subdetectors will be done during 2025, and the data taking period will start from 2026. LUXE will wrap up data taking by 2029, as the tunnel where LUXE is situated will be taken over by the XFEL facility by 2030.

## Acknowledgments

We thank the DESY technical staff for continuous assistance and the DESY directorate for their strong support and the hospitality they extend to the non-DESY members of the collaboration. This work has benefited from computing services provided by the German National Analysis Facility (NAF) and the Swedish National Infrastructure for Computing (SNIC).

## References

- [1] A. Gonoskov *et al.*, “Charged particle motion and radiation in strong electromagnetic fields,” *Rev. Mod. Phys.*, vol. 94, no. 4, p. 045001, 2022.
- [2] A. Fedotov *et al.*, “Advances in QED with intense background fields,” 2022.
- [3] C. Bamber *et al.*, “Studies of nonlinear QED in collisions of 46.6-GeV electrons with intense laser pulses,” *Phys. Rev. D*, vol. 60, p. 092004, 1999.
- [4] H. R. Reiss, “Production of electron pairs from a zero-mass state,” *Phys. Rev. Lett.*, vol. 26, pp. 1072–1075, 1971.
- [5] K. Poder *et al.*, “Experimental Signatures of the Quantum Nature of Radiation Reaction in the Field of an Ultraintense Laser,” *Phys. Rev. X*, vol. 8, no. 3, p. 031004, 2018.

- [6] J. M. Cole *et al.*, “Experimental evidence of radiation reaction in the collision of a high-intensity laser pulse with a laser-wakefield accelerated electron beam,” *Phys. Rev. X*, vol. 8, no. 1, p. 011020, 2018.
- [7] N. V. Zamfir, “Extreme Light Infrastructure Nuclear Physics (ELI-NP): Present status and perspectives,” *EPJ Web Conf.*, vol. 117, p. 10001, 2016.
- [8] H. Abramowicz *et al.*, “Letter of Intent for the LUXE Experiment,” 2019.
- [9] H. Abramowicz *et al.*, “Conceptual design report for the LUXE experiment,” *Eur. Phys. J. ST*, vol. 230, no. 11, pp. 2445–2560, 2021.
- [10] A. Hartin, A. Ringwald, and N. Tapia, “Measuring the Boiling Point of the Vacuum of Quantum Electrodynamics,” *Phys. Rev. D*, vol. 99, no. 3, p. 036008, 2019.
- [11] “XFEL: The European X-Ray Free-Electron Laser. Technical design report,” 2006.
- [12] “Expression of Interest for an ALICE ITS Upgrade in LS3,” 2018.
- [13] TowerJazz, “Official website,” <https://towersemi.com/>.